ACS OMEGA

Open Access

http://pubs.acs.org/journal/acsodf

Article

Efficient Water-Soluble Cu(II) Complex-Immobilized Electrospun Hydrophobic Polycaprolactone Nanofiber Composites for Highly Controlled and Long-Term Release

Maira Khalid, Muhammad Adnan, Muhammad Farooq, Yabuta Yoshinori, Jeongjin Park, Azeem Ullah, Gopiraman Mayakrishnan,* and Ick Soo Kim*

Cite This: *ACS Omega* 2025, 10, 12961−12971

Read Online

ACCESS | Metrics & More | Article Recommendations | Supporting Information

ABSTRACT: Water-soluble Cu complexes offer diverse applications in the biomedical field as Cu is an essential trace element for many physiological functions, including the wound healing process. Controlled delivery of such bioactive Cu complexes to the target system is a promising approach in biomedical applications. Herein, water-soluble Cu(II)−Schiff base complex-incorporated PCL nanofiber composites (PCL@C−1%, PCL@C−3%, and PCL@C−5%) were fabricated by the electrospinning process using a green solvent, acetic acid. Physicochemical properties of the resultant composite nanofibers were investigated by FE-SEM, EDS, TEM, UV−vis, FT−IR, XRD, TGA, BET, and XPS analyses. The successful incorporation of the Cu(II) complex into the PCL nanofiber was confirmed. Water contact angle (WCA) values revealed the hydrophobic nature of the PCL-composite nanofibers, which is also quite beneficial in the wound-healing process as it can create a hydrophobic barrier to prevent extra fluid absorption. To our delight, the release behavior of Cu complexes from the composite nanofibers was found to be gradual, highly controlled, and long-term release (up to 40 days). In addition, the resultant PCL composites demonstrated excellent antibacterial activity against both Gram-positive and Gram-negative bacteria. Overall, these findings provide significant insights into these Cu complex-incorporated PCL nanofiber membranes as potential antibacterial and long-term wound dressings.

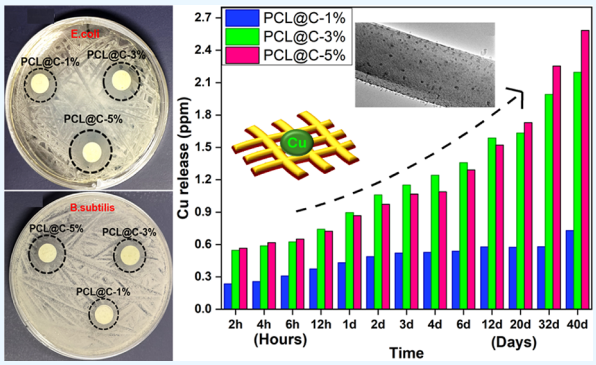

1. INTRODUCTION

Electrospinning has emerged as a simple and straightforward technique for producing ultrafine fibers, and it has been extensively employed for the development of nanofiber-based multifunctional membranes for various potential applications.[1] The characteristics of electrospun fibers, such as a high inherent surface-to-volume ratio, high porosity with small pores, tunable surface, and ability to be customized, make them excellent candidates in catalysis, energy, sensors, filtration, and biomedical applications.[2−4] Nanostructure-mediated drug delivery, a crucial technology in nanomedicine, has the potential to enhance drug bioavailability, enable long-term release of drug molecules, and facilitate precision drug targeting.[5] It is estimated that bacterial infections could contribute to approximately 10 million deaths by 2050, and to cope with this situation, new antibiotics are needed.[6,7] The electrospun nanofibers are found to be excellent candidates for controlled drug release.[8] Skin is highly vulnerable to damage from external threats.[9] Wounds typically heal through a finely balanced, efficient, and orderly sequence of repair events.[10] However, dysregulation can lead to chronic nonhealing ulcers.[11] Each year in the United States, wounds impact more than 6 million individuals, resulting in a financial burden of approximately 25 billion dollars and placing a substantial financial strain on the healthcare system.[12,13] The purpose of wound dressing is also the protection from the invasion of harmful microorganisms.[14−16] Hence, preventing wound infection caused by bacterial intrusion is a critical issue in the healing process.[17,18]

Copper is an essential trace element that is involved in numerous physiological processes across all body tissues. Copper is well-known for its antimicrobial properties, effective against all wound pathogens and resistant bacteria.[19,20] It also functions as an antiseptic and antimicrobial agent.[21] Delivering copper ions to the wound site is likely to enhance antibacterial effects and promote wound healing.[22,23] Under controlled release conditions, copper is crucial in the healing process by boosting the production of extracellular matrix molecules like

Received: October 11, 2024
Revised: February 26, 2025
Accepted: March 4, 2025
Published: March 25, 2025

Scheme 1. Schematic Showing the (a) Preparation of the Ligand and Water-Soluble Cu Complex, and the (b) Fabrication of Electrospun PCL@C Nanofibers (Scheme 1b, Right Side; SEM Image of the PCL@C Nanofiber)

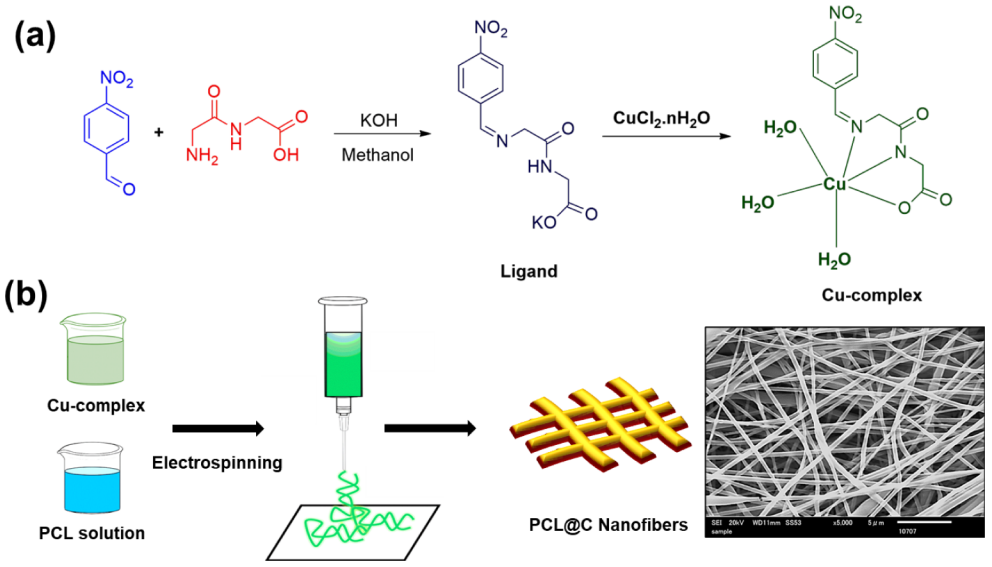

fibrinogen and collagen, which are essential for maintaining cell attachment and matrix integrity.[24,25] Among antibacterial metals, copper is particularly noteworthy for its capacity to balance potent antibacterial efficacy with excellent biocompatibility. In vivo studies have demonstrated a low risk of adverse reactions following direct skin contact with copper.[26,27] The U.S. Environmental Protection Agency (EPA) has approved the registration of antimicrobial copper.[28]

The clinical effectiveness of cisplatin has sparked interest in discovering new metal complexes for treating various diseases. For instance, researchers have created gold complexes aimed at addressing rheumatoid arthritis, silver complexes for their antimicrobial properties, and antimony complexes to combat leishmaniasis. Current clinical trials are investigating new therapeutic agents, including third-generation metal complexes. These examples illustrate the long-standing significance of therapeutic metal complexes and suggest a promising future for the field of inorganic medicine.[29] The water-soluble metal complexes (particularly, Cu complexes with Schiff base ligands) are potentially biologically important and can be used in various biomedical applications.[30] However, the controlled and long-term release of such bioactive Cu complexes to the target system is the key factor for achieving the best outcomes. Copper(II) complexes have shown remarkable promise in antibacterial and wound healing treatments, often outperforming silver and zinc. Their strength lies in their diverse mechanisms of action, including the production of reactive oxygen species (ROS), which effectively break down bacterial membranes, proteins, and DNA, providing broad-spectrum antibacterial effects. But their benefits go beyond fighting bacteria. Copper(II) complexes actively support wound healing by promoting the growth of new blood vessels (angiogenesis) and boosting collagen production, both of which are essential for tissue repair. Additionally, their ability to form stable complexes allows for controlled drug delivery, making them a versatile and powerful tool in therapeutic applications.[31−33]

Copper-complex nanofiber dressings are gaining attention as practical and effective alternatives to silver-based dressings. Not only do they match—or even exceed—the antibacterial and wound-healing properties of silver dressings, but they also offer additional benefits. Copper dressings are more affordable, less toxic to human cells, and particularly good at breaking down biofilms, which are major challenges in treating chronic wounds. They also offer controlled drug release and better mechanical strength, making them ideal for long-term wound care. While popular silver dressings like Acticoat and Aquacel Ag are highly effective, copper-based dressings provide a more cost-effective option without compromising on performance, making them an exciting development in wound treatment.[34,35]

The polycaprolactone (PCL), a semicrystalline synthetic polymer, has been extensively studied for sustained drug delivery applications. PCL nanofibrous scaffolds loaded with antibacterial agents have demonstrated sustained release profiles and stability for several months.[36] It is a polymer approved by the Food and Drug Administration (FDA), known for its chemical stability, biocompatibility, biodegradability, affordability, and ease of electrospinning[37,38] We presumed that the immobilization of biologically active water-soluble Cu complexes into the electrospun PCL nanofiber would be an excellent approach to develop an efficient membrane for biomedical applications.

Herein, a facile one-step electrospinning process was opted to develop a novel water-soluble Cu(II) complex-incorporated PCL nanofiber membrane. Glacial acetic acid was used as a green electrospinning solvent. Green solvents are paving the way for more sustainable and practical approaches to materials science. Unlike traditional solvents, such as dichloromethane, dimethylformamide, and chloroform, green solvents offer a safer and more environmentally friendly option, especially for large-scale production. The problem with these conventional solvents is their toxicity and the health risks they pose, making them less ideal for commercial applications. On top of that, using them often requires extra steps, such as washing and vacuum treatments, to ensure the materials are safe and usable, which adds complexity and cost. Embracing greener alternatives not only addresses these issues but also opens up new possibilities for creating nanofiber-based materials that are both high-performing and eco-friendly.[39,40] To the best of our knowledge, this work represents the first development of

https://doi.org/10.1021/acsomega.4c09305
ACS Omega 2025, 10, 12961−12971

electrospun nanofiber composites incorporating water-soluble metal complexes. Polycaprolactone (PCL) nanofibers with varying weight percentages of water-soluble copper complexes were successfully fabricated. The resulting nanofiber membranes were thoroughly characterized using a range of physicochemical and thermal analysis techniques, including SEM, FE-SEM, TEM, XRD, FT-IR, and TGA. The surface wetting behavior of the composite nanofibers was evaluated through water contact angle (WCA) analysis. UV−vis spectroscopy and XPS analysis further confirmed the successful integration of copper complexes into the PCL nanofiber matrix. The copper release behavior of the fabricated membranes was assessed by using ICP-OES analysis, while their antimicrobial activity was systematically investigated, demonstrating the multifunctional potential of these innovative nanofiber composites.

2. EXPERIMENTAL PROCEDURE

2.1. Materials. Polycaprolactone (PCL, Mw = 80 kDa), glycylglycine (GG), 4-nitrobenzaldehyde, Cu(II) chloride salt ($CuCl_2$), and potassium hydroxide pellets (KOH) were obtained from Sigma-Aldrich, Japan. Glacial acetic acid (>99.7%) was sourced from Fujifilm Wako Pure Chemicals Ltd., Japan. The 2,2-diphenyl-1-picrylhydrazyl (DPPH) antioxidant assay kit was acquired from Dojindo Laboratories, Kumamoto, Japan. The bacterial strains *Escherichia coli* (*E. coli*) BW25113 and *Bacillus subtilis* (*B. subtilis*) 168 were kindly provided by the Gene Research Center at Shinshu University, Ueda. Petri dishes were obtained from Sansei Medical Co., Ltd., Japan. Milli-Q water (Direct-Q UV3) was used in all of the experiments. All chemicals were used as received without further purification.

2.2. Synthesis of Cu(II) Schiff Base Complex. The Cu(II) complex was prepared using the previously reported procedure.[30] Briefly, a mixture of GG (5 mmol), KOH (5 mmol), and methanol (25 mL) was prepared in a round-bottom flask (Scheme 1a). On the other hand, 4-nitrobenzaldehyde (5 mmol) was dissolved in 25 mL of methanol, and the solution was added dropwise to the above-prepared mixture in a round-bottom flask while stirring the solution at room temperature. After the dropwise addition, the temperature of the reaction mixture was raised to 60 °C, and stirring was continued for 8 h. A solution of $CuCl_2$ (5 mmol) in aqueous methanol (25 mL) was gradually added to the reaction mixture and continuously stirred for 2 h. The pale-green precipitate was obtained, filtered, and washed with cold ethanol and diethyl ether. Finally, the samples were dried in a vacuum over anhydrous $CaCl_2$. The successful preparation of the Cu(II) complex was confirmed by FT-IR analysis (Figure S1); FT-IR (cm^{-1})[$CuL(H_2O)_3$], $C_{11}H_{15}CuN_3O_8$: 1640 ($\nu_{azo.}$ (C = N)), 1606 ($\nu_{asym.}(COO^-)$), 1380 ($\nu_{sym.}(COO^-)$), 3352 ($\nu(H_2O)$), 580 (ν(M-O)), and 424 (ν(M-N)).[29]

2.3. Preparation of Cu(II) Complex Immobilized PCL Nanofibers. The 35 wt % PCL spinning solution was prepared in a mixture of 90% glacial acetic acid and 10% water. The solution was stirred for 24 h on a magnetic stirrer at 600 rpm and 60 °C to ensure homogeneity. For electrospinning, a horizontal arrangement of a high-voltage power supply (Har-100*12, Matsusada Co., Tokyo, Japan), a rotating cylindrical collector, and a syringe pump (KDS-100, KD Scientific, USA) was set up. The spinning solution was loaded into a 20 mL plastic syringe equipped with a 20-gauge needle (0.9 mm diameter). A high voltage of 21 kV was applied at the needle tip with a flow rate of 0.8 mL/h. The distance between the needle tip and collector was maintained at 200 mm. The nanofibrous mat was collected on a piece of butter paper wrapped around the collector. Electrospinning was carried out at an ambient temperature of 25 °C and a relative humidity of 40%. To produce composite PCL@C nanofibers, a Cu(II) complex was added to the above formulation in concentrations of 1%, 3%, and 5% by weight relative to the polymer (Scheme 1b). The resulting nanofibers were labeled as PCL, PCL@C−1%, PCL@C−3%, and PCL@C−5%. The processing parameters for blending PCL@C nanofibers were the same as those for neat PCL.

2.4. Characterization. The surface morphology and nanofiber diameter were studied by using scanning electron microscopy (SEM, JSM-6010LA, JEOL, Japan). Prior to imaging, the nanofiber samples were sputter-coated with platinum. Fifty nanofibers were randomly selected from the SEM images, and their diameters were measured and averaged to determine the mean nanofiber diameter. SEM micrographs were analyzed by using ImageJ software (version 1.4.3). Field emission scanning electron microscopy (FE-SEM, JSM-IT800SHL) and high-resolution transmission electron microscopy (TEM, JEOL, JEOL2010, 200 kV accelerating voltage) were employed to examine the morphology and elemental composition of the membrane. The physicochemical properties of the produced nanofiber mats were analyzed using Fourier-transform infrared spectroscopy (FTIR, Prestige-21 instrument, Shimadzu Co., Ltd., Japan). Powder X-ray diffraction data were collected on an X-ray diffractometer using Cu−Kα radiation with a wavelength of 1.5406 Å, equipped with nickel-filtered CuKα radiation (Rotaflex RT300 mA, Rigaku Co., Osaka, Japan). Thermal degradation analysis of the PCL and Cu complex immobilized nanofiber membranes was conducted using thermogravimetric analysis (TGA) on a TG-8120 instrument from Rigaku, Japan. The sample was subjected to thermal degradation from 30 to 600 °C in an air atmosphere with a temperature ramp rate of 10 °C/min. The Brunauer−Emmett−Teller (BET) specific surface area (SSA) and pore size distribution of electrospun nanofiber membranes of PCL and Cu complex immobilized PCL were analyzed using nitrogen (N_2) physisorption with a SHIMADZU Tri-Star II-3020 instrument (Japan). Each specimen, weighing 300 mg, was degassed at 80 °C for 1 h under nitrogen.[41] The wetting behavior of the PCL and composite PCL@C (1%, 3%, and 5%) nanofiber membranes was evaluated using a contact angle analyzer, specifically the Digidrop instrument from GBX, Whitestone Way, France. A static water contact angle was measured by using a 28-gauge needle. Five readings were taken for each type of nanofiber membrane, and the mean contact angle was calculated from these measurements. Ultraviolet−visible (UV−vis) absorption spectra of Cu complex immobilized PCL nanofiber membranes were obtained using a UV−vis spectrophotometer (1800, Shimadzu Japan). The spectra were recorded before and after 30 days of immersion in a PBS solution. X-ray photoelectron spectroscopy (XPS) analysis was conducted by using an AXIS-ULTRA HSA SV instrument to comprehensively characterize the chemical structure and surface morphology of PCL@C (1%, 3%, and 5%) nanofiber membranes. Inductively coupled plasma optical emission spectrometry (ICP-OES, SPS 5000) was used to study the release behavior.

2.5. Release Behavior. Copper release from the electrospun PCL@C (1%, 3%, and 5%) nanofiber membranes was

https://doi.org/10.1021/acsomega.4c09305
ACS Omega 2025, 10, 12961−12971

quantified using ICP-OES. To assess the release behavior, 300 mg of nanofiber mats was immersed in 20 mL of phosphate-buffered saline (PBS, pH 7.2−7.4) within glass bottles placed in a 37 °C incubator. At predetermined intervals spanning 0 h to 40 days, 1 mL of the solution was withdrawn and analyzed for copper content using ICP-OES. Simultaneously, an equivalent volume of fresh PBS was added to maintain constant sink conditions, ensuring accurate measurement of copper release over time.

2.6. Antibacterial Activity. The qualitative antibacterial activity of electrospun PCL@C (1%, 3%, and 5%) nanofiber membranes was evaluated using the agar plate disc diffusion method (AATCC 147−1998), as previously described.[16] Overnight cultures of Gram-negative *Escherichia coli* and Gram-positive *Staphylococcus aureus* were diluted to a 10−5 concentration, and 50 μL aliquots were spread evenly on agar plates. Circular discs, 10 mm in diameter, were cut from the nanofiber mats and gently pressed onto the agar surface to ensure good contact. The plates were then incubated at 37 °C for 24 h. Following incubation, the plates were examined for bacterial growth inhibition both directly underneath the discs and within the zones of inhibition surrounding them. This method allowed for the qualitative assessment of the nanofiber membranes' effectiveness against bacterial strains.

3. RESULTS AND DISCUSSION

3.1. Physicochemical Properties of PCL@C Nanocomposites. The neat PCL and Cu complex-incorporated electrospun composite nanofibers were successfully synthesized with different wt % (1%, 3%, and 5%) of Cu complex with respect to polymer concentration. The surface morphology of the PCL@C nanocomposites was studied by SEM, FE-SEM, and TEM analysis. The micrographs and fiber diameter histogram of prepared PCL@C nanofibers are depicted in Figures 1 and S2. All the nanofiber mats showed very smooth,

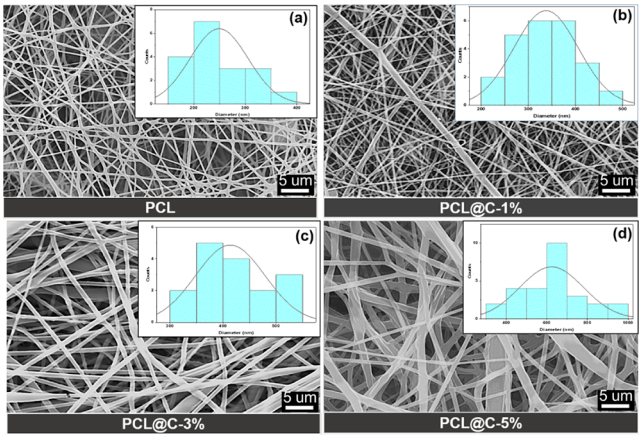

Figure 1. SEM micrographs and their diameter distribution graphs of the nanofiber composites. (a) PCL, (b) PCL@C−1%, (c) PCL@C−3%, and (d) PCL@C−5%.

uniform, and beadless nanofiber surface morphology. The fiber diameter was observed to be significantly increased with the wt % of the Cu complexes. The diameter of PCL nanofiber mats was calculated to be in the range of 150−400 nm, whereas after the incorporation of the Cu complex into the PCL nanofibrous scaffold, the diameter significantly increased. The incorporation of copper complexes into the polymer solution increases its viscosity, which directly impacts the dynamics of the electrospinning process. Higher viscosity limits the elongation and thinning of the jet during spinning, resulting in the formation of thicker fibers. This highlights the importance of optimizing solution viscosity to achieve the desired fiber morphology in nanofiber composites.[42] The fiber diameter of PCL@C−1%, PCL@C−3%, and PCL@C−5% was determined to be in the range of 200−600, 300−625, and 350−1000 nm, respectively. This phenomenon is mainly due to the change in the viscosity and conductivity of the PCL/Cu-complex spinning solution.

To further evaluate, the prepared nanofiber membranes were analyzed by FE-SEM and EDS (Figures 3 and S3 and S4). The FESEM micrographs (inset; EDS Cu-elemental mapping) of PCL and Cu complex-incorporated PCL nanofiber membranes are depicted in Figure 2. Like the SEM results, the FE-SEM

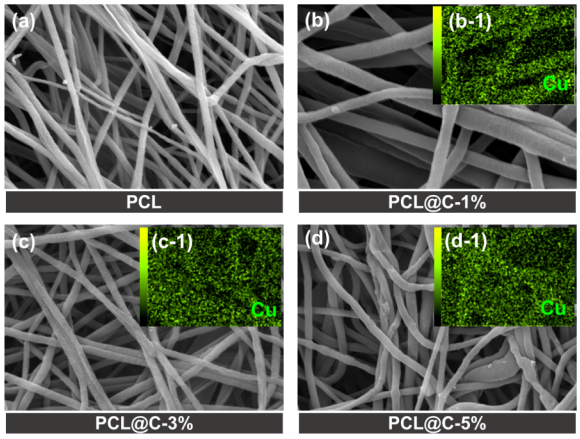

Figure 2. FESEM micrographs of the nanofiber composites. (a) PCL, (b) PCL@C−1%, (c) PCL@C−3%, and (d) PCL@C−5%, and the insets (b-1, c-1, and d-1) are elemental mapping of Cu. The scale bar is 200 nm.

images of neat PCL nanofibers showed an almost smooth and uniform morphology (Figure 2a). Similarly, PCL@C-1% membranes exhibited an almost smooth morphology, but as the amount of Cu complex increases, the nanofibers become intertwined, as clearly visible in Figure 2c,d. Fiber diameter also increases as the Cu complex concentration increases. The EDS spectra were recorded for the composite nanofibers. The results confirm the presence of the Cu element in all three samples, PCL@C−1%, PCL@C−3%, and PCL@C−5% (Figure 3b-1, c-1 and d-1). Moreover, the homogeneous distribution of Cu in the samples was also confirmed. No Cu element was detected for the pure PCL nanofiber (Figure S4).

In order to investigate the homogeneous distribution of Cu complexes in the PCL nanofiber matrix in detail, TEM images were recorded for all four samples (Figure 3). The TEM micrographs of neat PCL, PCL@C−1%, PCL@C−3%, and PCL@C−5% are shown in Figure 3.

Neat PCL nanofiber exhibited a smooth surface without any Cu complexes, as shown in Figure 3a, while all other Cu-complex-incorporated nanofiber membranes showed the presence of particle-like Cu-complexes in the nanofibers (Figure 3b,c,d). The increase in the loading wt % of the Cu complex resulted in more complex particles in the nanofiber membranes. The PCL@C−1% and PCL@C−3% composites show a uniform dispersion of Cu complexes, whereas the

https://doi.org/10.1021/acsomega.4c09305
ACS Omega 2025, 10, 12961−12971

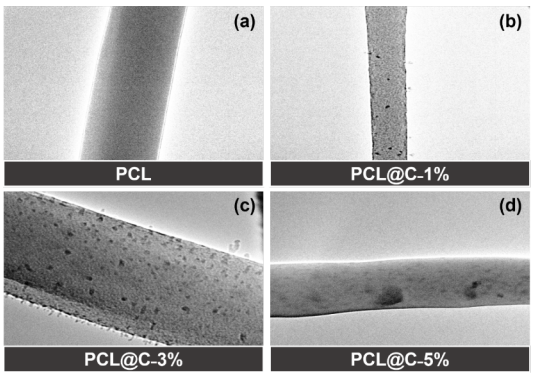

Figure 3. TEM images of nanofiber composites, (a) PCL, (b) PCL@C−1%, (c) PCL@C−3%, and (d) PCL@C−5%. The scale bar is 200 nm.

PCL@C−5% composite demonstrated some aggregation of Cu complexes in the PCL nanofibers.

The structural properties of the PCL nanofibers before and after immobilization of Cu complexes were investigated by FT-IR and XPS analysis (Figure 4). The FT-IR spectra of neat PCL and Cu complex-incorporated PCL nanofiber membranes are exhibited in Figure 4a. The FT-IR spectrum of the PCL nanofibers reveals distinct absorption bands. The dominant peaks at 2946 and 2868 cm^{-1} correspond to the asymmetric and symmetric stretching vibrations of the CH_2 groups, respectively. The carbonyl group (C═O) was observed at 1745 cm^{-1}. The peak at 1366 cm^{-1} represents the bending vibration of the CH_2 groups, and the C−C stretching vibration is identified at 1236 cm^{-1}.[43,44] After the incorporation of the Cu complex, a significant increase in the intensity of peaks was clearly noticed, which may be due to the enhancement in the crystalline nature of the composite PCL membranes. Although there is no additional peak related to the Cu complex, this might be due to the structural similarity of the PCL and Cu complex. The XPS analysis was conducted to investigate the structure and chemical states of elements present in the PCL, PCL@C−1%, PCL@C−3%, and PCL@C−5% nanofiber membranes (Figure 4b,c,d). As expected, the XPS spectra of pure PCL nanofibers showed only two dominant peaks corresponding to the C 1s and the O 1s peaks (data not shown). The XPS survey spectra of PCL@C−1%, PCL@C−3%, and PCL@C−5% demonstrate the successful incorporation of the Cu complex in PCL nanofibers. As we can see in Figure 4c,d, there are characteristic peaks of Cu at around 942 and 963 eV attributed to Cu $2p_{3/2}$ and Cu $2p_{1/2}$, respectively. The PCL@C−1% sample showed very weak peaks corresponding to Cu, which might be due to the very low amount or excellent dispersion of the Cu complex in the PCL nanofiber matrix. The intensity of the XPS Cu $2p_{3/2}$ and Cu $2p_{1/2}$ core peaks was noticed to be significantly increased with the wt % of Cu-complexes. The results confirm the successful immobilization of the Cu complex in the PCL nanofibers.

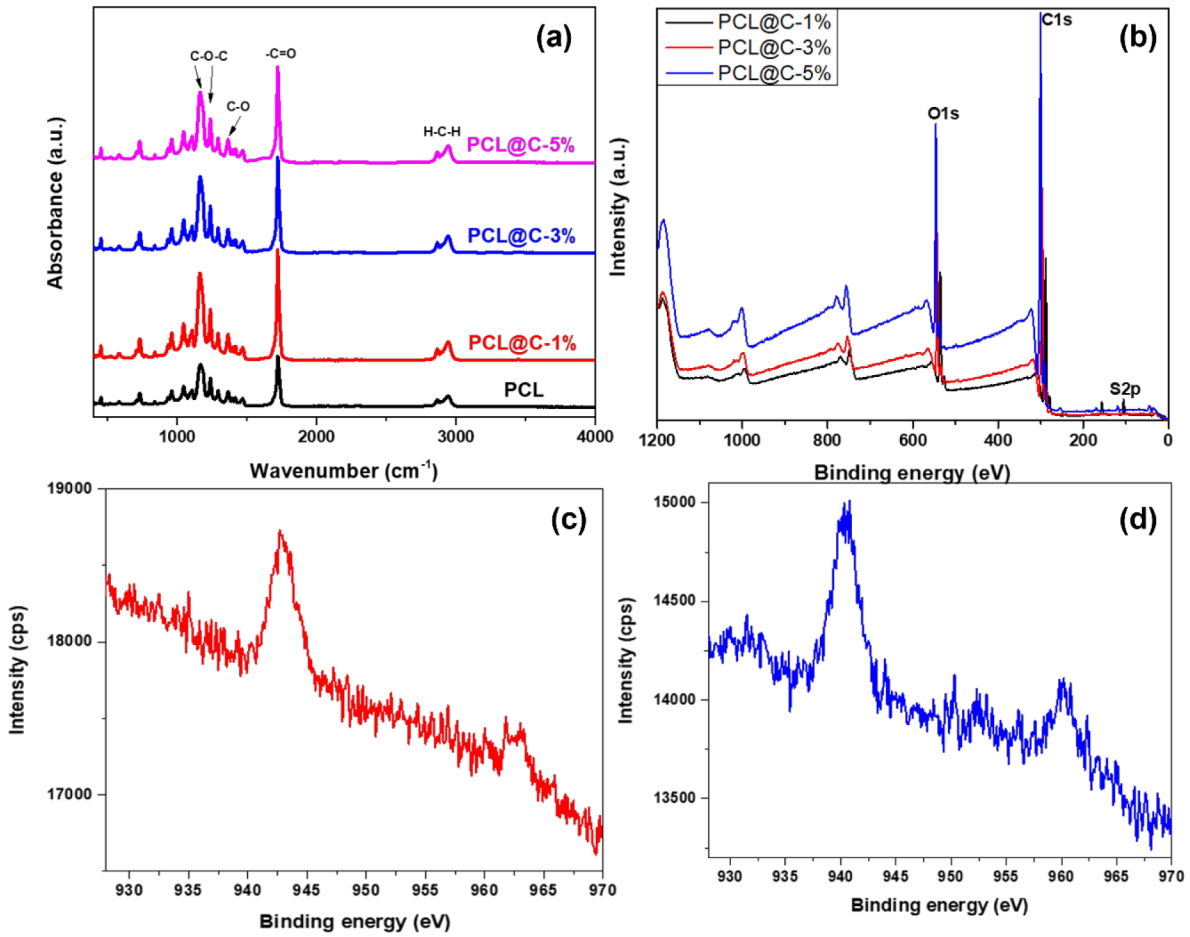

Figure 4. (a) FT-IR spectra and (b) XPS survey spectra of PCL, PCL@C−1%, PCL@C−3%, and PCL@C−5%, and the XPS high-resolution Cu 2p peaks of (c) PCL@C−3% and (d) PCL@C−5%.

https://doi.org/10.1021/acsomega.4c09305
ACS Omega 2025, 10, 12961−12971

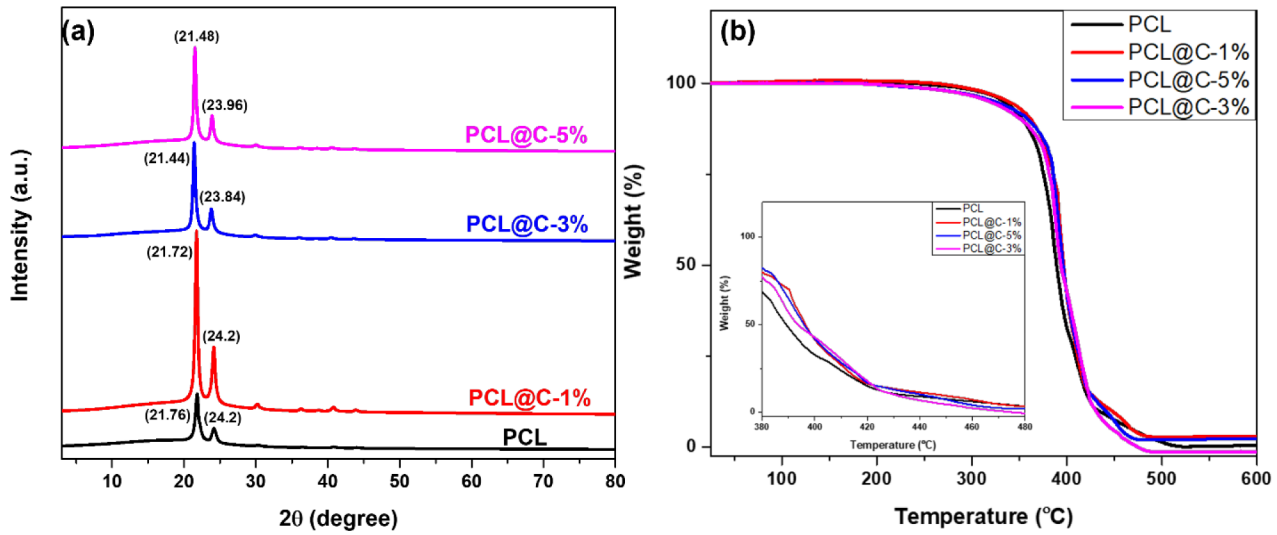

Figure 5. (a) XRD patterns and (b) TGA curves of PCL, PCL@C−1%, PCL@C−3%, and PCL@C−5%.

3.2. Crystalline Nature of PCL@C Nanocomposites. The crystallinity of nanofibers has a significant influence on the mechanical properties of the membrane. Higher crystallinity correlates with higher mechanical strength, which is important for wound dressing applications.[45] The XRD spectra for neat PCL nanofiber membranes and Cu complex-incorporated PCL membranes (PCL@C−1%, PCL@C−3%, and PCL@C−5%) are depicted in Figure 5a. All nanofiber membranes exhibited two strong peaks at 2θ = 21.5° and 23.5°, corresponding to (110) and (120) planes, within the 2θ range of 5−80°, indicative of their semicrystalline nature.[46] After the immobilization of the Cu complex, the intensity of the two main peaks (2θ = 21.5° and 23.5°) increased. Moreover, there is no strong peak relevant to the Cu complex, which is indicative that the Cu complex is well dispersed in the polymer solution, and the semicrystalline structure of PCL is also significantly increased.[47,48] If we closely look at the XRD spectrum, we can see the very weak peaks around 2θ = 30°, 36°, and 41° that correspond to (104), (012), and (110) planes that might be related to the Cu complex. The XRD results are in good agreement with the FT-IR results.

3.3. Thermal Property of PCL@C Nanocomposites. The thermal stability of nanofibrous membranes is important to withstand exposure to heat, thus preventing the wounded area from harm.[49] The TGA curves were obtained to further investigate the prepared nanofibrous membranes. The TGA curves of neat PCL, PCL@C−1%, PCL@C−3%, and PCL@C−5% nanofibers are shown in Figure 5b. Two decomposition stages can be seen that are around 330 and 410 °C, and at this point, there is a visible difference in weight loss of all prepared nanofiber membranes. The maximum weight loss at 380 °C was observed for PCL nanofiber membranes, which was around 32%, and the minimum weight loss was observed for PCL@C-5% nanofiber membranes, which was around 18%. Additionally, all TGA curves are not the same as PCL, which is indicative of the interaction between PCL and the Cu complex, due to which the thermal properties of the nanofiber membranes changed slightly.[50]

3.4. BET Surface Area of PCL@C Nanocomposites. Electrospun nanofiber membranes that possess a high specific surface area create an ideal environment for the intricate and dynamic process of wound healing. These membranes offer numerous sites for the incorporation of wound healing agents and serve as an effective platform for drug delivery.[51] The BET analysis was performed to determine the surface area of the prepared neat PCL and Cu complex-incorporated PCL nanofiber membranes (PCL@C−1%, PCL@C−3%, and PCL@C−5%). The surface area of all nanofiber membranes is presented in Table S1. The surface area of pristine PCL membrane is found to be 4.05 m^2/g, whereas the surface area for PCL@C-1% and PCL@C-3% is 5.23 and 7.20 m^2/g, respectively. The increase in the surface area may be due to the smaller diameter of the nanofiber and the huge dispersion of the Cu complex in the PCL nanofiber. However, the BET surface area for PCL@C-5% is determined to be slightly lower at 2.43 m^2/g, which is mainly due to the larger fiber diameter and aggregation of the Cu complex. When the surface area decreases, it can limit how much drug the material can hold and slow its release, which might reduce its effectiveness. However, this challenge can be tackled by fine-tuning the material's porosity and surface properties; by doing so, it is possible to keep the performance intact—or even improve it—despite the reduced surface area.[52] The BET result is in good agreement with the SEM, FE-SEM, and TEM observations.

3.5. Hydrophobic Nature of PCL@C Nanocomposites. The hydrophobicity of nanofibers greatly controls blood wetting and bacterial adhesion to the wound site, thus helping in homeostasis and wound healing properties.[53] The wettability of the prepared nanofiber membranes was investigated by water contact angle (WCA) measurement, and the results are depicted in Figure 6. PCL is a hydrophobic polymer with a very high contact angle.[54,55] It can be seen in Figure 6 that PCL showed a WCA of 123°, and after the incorporation of the Cu complex, the wettability of the prepared fibers increased significantly, and the WCA dropped to 102.8°. This is due to the incorporation of the water-soluble Cu complex in the PCL nanofibers. The WCA was found to decrease with the concentration of the Cu complex.

3.6. Release Behavior of PCL@C Nanocomposites. Electrospinning offers great flexibility in selecting materials and drugs for drug delivery applications compared with other techniques. The ability of electrospun fibers to modulate drug release is a significant advantage for these applications.[56] PCL is known for its nonswellable nature and slow degradation rate

https://doi.org/10.1021/acsomega.4c09305
ACS Omega 2025, 10, 12961−12971

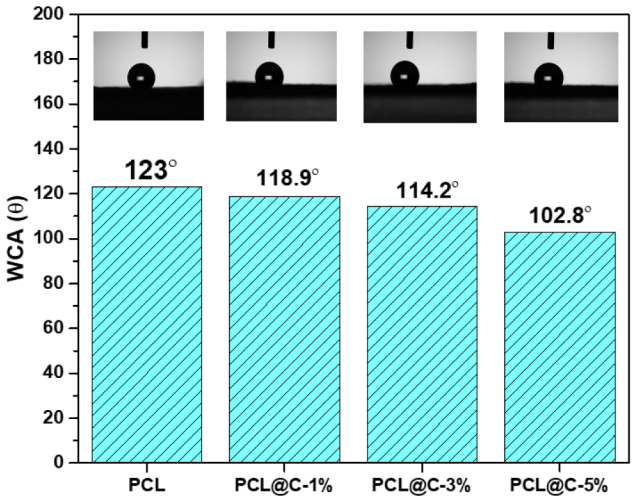

Figure 6. Water contact angles of PCL, PCL@C−1%, PCL@C−3%, and PCL@C−5%.

in phosphate-buffered saline (PBS). These characteristics eliminate the possibility of swelling or chemically controlled drug release mechanisms. Consequently, it is presumed that the controlled release mechanism in PCL membranes is primarily diffusion-controlled.[57] In general, hydrophobic polymers like PCL regulate drug diffusion by reducing the initial burst release and enabling sustained delivery. The strong drug-polymer interactions embed the drug within the matrix, further controlling the release. As noted by Kamaly et al.,[58] drug release occurs through diffusion and polymer erosion, ensuring prolonged and steady delivery.[59]

The release behavior of the present PCL@C−1%, PCL@C−3%, and PCL@C−5% nanofiber membranes is shown in Figure 7a,c. The PCL nanofiber membranes containing varying quantities of Cu complex, such as 1, 3, and 5 wt %, exhibited almost similar release behavior. The release is very controlled and steady, even over a period of 40 days for all nanofiber membranes. Additionally, none of the electrospun nanofiber membranes exhibited a high burst release, indicating optimal encapsulation of the drug within the fibers. The release data were further analyzed using different release kinetic models as described by previous reports.[60] The release data showed a better fit with the Korsmeyer−Peppas model with R^2 values of 0.9777 and 0.9989 for days and hours, respectively, as shown in Figure S6 and the slope of curve value (n) of 0.234 and 0.138 indicates that the drug release mechanism was Fickian diffusion as the value of n is smaller than 0.45.[61]

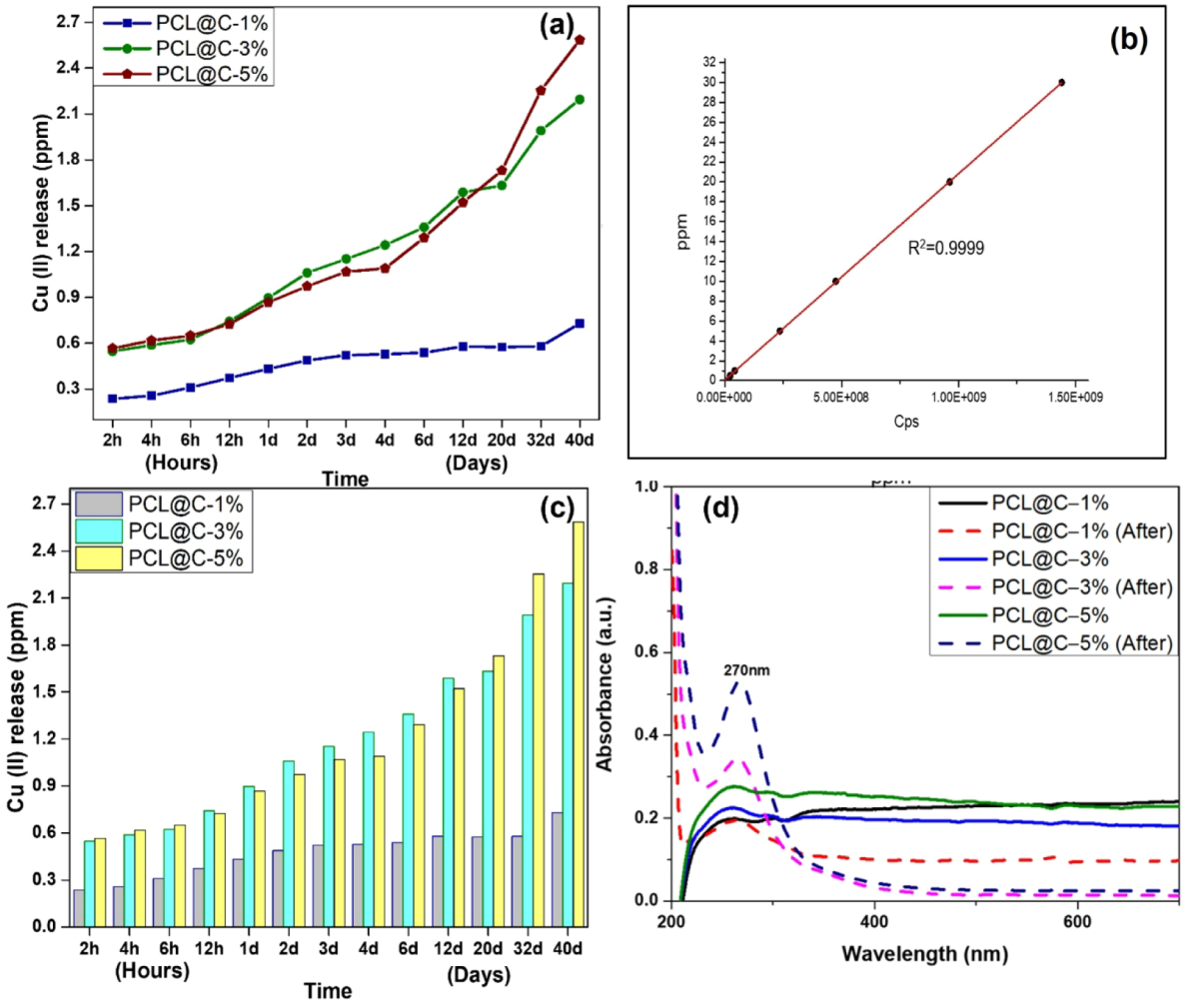

Figure 7. Release behavior of Cu complex-incorporated nanofiber membranes: (a, c) release behavior for 40 days, (b) standard curve, and (d) UV−vis spectra of prepared nanofiber composites before and after immersion in PBS solution for 30 days.

https://doi.org/10.1021/acsomega.4c09305
ACS Omega 2025, 10, 12961−12971

The copper release was well-defined by ICP-OES, and in order to understand the release of Cu in the form of a complex, UV−vis was performed. Figure 7d shows the UV spectra of Cu complex-incorporated PCL nanofiber membranes after immersion in PBS solution at different time intervals (2 h and 30 days). There is no peak after 2 h immersion in PBS solution because the Cu complex is intactly distributed in the PCL nanofibers. However, the UV−vis spectra after 30 h of immersion show a clear peak around 275 nm, which indicates the release of Cu is in the form of a Cu complex.[62]

3.7. Antibacterial Activity of PCL@C Nanocomposites. Bacterial infections play a crucial role in skin infections. Microorganisms primarily colonize the wounded area, delaying the inflammation process and extending healing time.[63] The antibacterial study was conducted on Cu complex immobilized PCL nanofiber membranes against Gram-negative *Escherichia coli* and Gram-positive *Bacillus subtilis* bacterial strains. These strains are known to be the primary source of soft tissue infections, which can significantly delay wound healing. Gram-positive bacteria are often responsible for many hospital-acquired infections, while *Escherichia coli* is commonly associated with infections in burn wounds.[64,65] The results of the antibacterial testing are depicted in Figure 8. Clear zones,

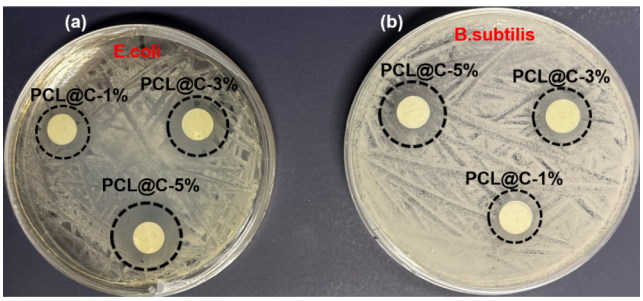

Figure 8. Antibacterial activity of prepared PCL@C−1%, PCL@C−3%, and PCL@C−5% against (a) *E. coli* and (b) *B. subtilis*.

or halos, indicating areas without bacterial growth, were observed around the Cu complex-incorporated PCL nanofiber discs, demonstrating the antibacterial effectiveness of the Cu complex against both Gram-positive and Gram-negative bacterial strains. Especially, the prepared nanofiber membranes are more effective against Gram-negative bacteria *E. coli* as the diameter of the zone of inhibition is bigger than that of *B. subtilis*. Similar observations were reported earlier. Additionally, as the concentration of the Cu complex in the composite nanofiber increased, the size of the clear zones also expanded, indicating enhanced antibacterial activity. Although the copper complex in PCL@C-5% was observed in an aggregated form, copper complexes are well-documented for retaining their bioactivity, even under such conditions. Their antibacterial efficacy is primarily driven by mechanisms such as oxidative stress induction and bacterial membrane disruption, which remain effective as long as the complexes interact with the bacterial environment. Additionally, the release kinetics of Cu ions, governed by the degradation rate of the PCL matrix, ensure a steady and sustained therapeutic effect. This controlled release prevents abrupt spikes in ion concentration, reducing the risk of resistance development and maintaining consistent antibacterial efficacy over time.[66,67]

Overall, the results confirm that the PCL composite nanofibers are hydrophobic in nature, with a high surface area, are thermally stable, and semicrystalline. The preparation process is simple and uses green solvents. These findings provide significant insights into these Cu complex-incorporated PCL nanofiber membranes as potential antibacterial and long-term wound dressings.

4. CONCLUSION

In summary, water-soluble Cu(II) complex-incorporated PCL nanofiber membranes were successfully fabricated by a simple electrospinning technique. Acetic acid was used as a green solvent for the electrospinning process. These prepared nanofiber membranes provided valuable insight into their potential applications in antibacterial wound dressing applications. The prepared nanofiber membranes showed uniform morphology for all samples, but a change in the diameter of the nanofibers was noticed with the amount of Cu complex. The homogeneous dispersion of the Cu complex is clearly seen in TEM micrographs. The FE-SEM and XPS results showed the presence of a Cu complex in the PCL nanofibers. The prepared nanofiber membranes are hydrophobic, and the PCL@C−5% showed a water contact angle of 102.8°. This property is potentially useful for creating a hydrophobic barrier that could prevent excessive moisture buildup. The release of Cu is very sustained and gradual for up to 40 days, which is very good for long-term wound dressing applications. Moreover, the antibacterial activity against Gram-negative and Gram-positive bacteria is also found to be excellent, especially for Gram-negative bacteria, where antibacterial activity is even stronger, which is extremely beneficial because Gram-negative bacteria cause wound and surgical site infections.

■ ASSOCIATED CONTENT

Supporting Information

The Supporting Information is available free of charge at https://pubs.acs.org/doi/10.1021/acsomega.4c09305.

FT-IR, EDS, elemental mapping, SEM, XPS and Korsmeyer−Peppas model fitting curves results are provided (PDF)

■ AUTHOR INFORMATION

Corresponding Authors

Gopiraman Mayakrishnan − *Nano Fusion Technology Research Group, Institute for Fiber Engineering and Science (IFES), Interdisciplinary Cluster for Cutting Edge Research (ICCER), Shinshu University, Ueda, Nagano 386-8567, Japan*; orcid.org/0000-0002-0137-8617; Email: kim@shinshu-u.ac.jp

Ick Soo Kim − *Nano Fusion Technology Research Group, Institute for Fiber Engineering and Science (IFES), Interdisciplinary Cluster for Cutting Edge Research (ICCER), Shinshu University, Ueda, Nagano 386-8567, Japan*; orcid.org/0000-0003-2126-0381; Email: gopiraman@shinshu-u.ac.jp

Authors

Maira Khalid − *Nano Fusion Technology Research Group, Institute for Fiber Engineering and Science (IFES), Interdisciplinary Cluster for Cutting Edge Research (ICCER), Shinshu University, Ueda, Nagano 386-8567, Japan*

Muhammad Adnan − *Nano Fusion Technology Research Group, Institute for Fiber Engineering and Science (IFES), Interdisciplinary Cluster for Cutting Edge Research (ICCER), Shinshu University, Ueda, Nagano 386-8567, Japan*

Muhammad Farooq − *Nano Fusion Technology Research Group, Institute for Fiber Engineering and Science (IFES), Interdisciplinary Cluster for Cutting Edge Research (ICCER), Shinshu University, Ueda, Nagano 386-8567, Japan*; orcid.org/0009-0001-3427-3918

Yabuta Yoshinori − *Nano Fusion Technology Research Group, Institute for Fiber Engineering and Science (IFES), Interdisciplinary Cluster for Cutting Edge Research (ICCER), Shinshu University, Ueda, Nagano 386-8567, Japan*

Jeongjin Park − *Nano Fusion Technology Research Group, Institute for Fiber Engineering and Science (IFES), Interdisciplinary Cluster for Cutting Edge Research (ICCER), Shinshu University, Ueda, Nagano 386-8567, Japan*; orcid.org/0000-0002-7167-151X

Azeem Ullah − *Nano Fusion Technology Research Group, Institute for Fiber Engineering and Science (IFES), Interdisciplinary Cluster for Cutting Edge Research (ICCER), Shinshu University, Ueda, Nagano 386-8567, Japan*

Complete contact information is available at: https://pubs.acs.org/10.1021/acsomega.4c09305

Author Contributions

The manuscript was prepared with contributions from all authors. All authors provided their approval for the final version of the manuscript.

Notes

The authors declare no competing financial interest.

■ ACKNOWLEDGMENTS

This paper is based on results obtained from a project, JPNP 22021, commissioned by the New Energy and Industrial Technology Development Organization (NEDO). We thank Prof. Karvembu Ramasamy, National Institute of Technology, Tiruchirappalli, India, for the support in investigating the metal complexes.

■ REFERENCES

(1) Huang, Z. M.; Zhang, Y. Z.; Kotaki, M.; Ramakrishna, S. A review on polymer nanofibers by electrospinning and their applications in nanocomposites. *Compos. Sci. Technol.* **2003**, *63*, 2223−2253.

(2) Zhao, S.; Li, L.; Wang, H.; Zhang, Y.; Cheng, X.; Zhou, N.; Rahaman, M. N.; Liu, Z.; Huang, W.; Zhang, C. Wound dressings composed of copper-doped borate bioactive glass microfibers stimulate angiogenesis and heal full-thickness skin defects in a rodent model. *Biomaterials* **2015**, *53*, 379−391.

(3) Ullah, A.; Ullah, S.; Khan, M. Q.; Hashmi, M.; Nam, P. D.; Kato, Y.; Tamada, Y.; Kim, I. S. Manuka honey incorporated cellulose acetate nanofibrous mats: Fabrication and in vitro evaluation as a potential wound dressing. *Int. J. Biol. Macromol.* **2020**, *155*, 479−489.

(4) Yang, S.; Li, X.; Liu, P.; Zhang, M.; Wang, C.; Zhang, B. Multifunctional Chitosan/Polycaprolactone Nanofiber Scaffolds with Varied Dual-Drug Release for Wound-Healing Applications. *ACS Biomater. Sci. Eng.* **2020**, *6* (8), 4666−4676.

(5) Chellamani, K. P.; Balaji, R. S. V.; Veerasubramanian, D.; Sudharsan, J. Wound healing ability of herbal drug incorporated PCL (Poly (ε-caprolactone)) wound dressing. *J. Acad. Ind. Res.* **2014**, *2*, 622−626.

(6) Mulani, M. S.; Kamble, E. E.; Kumkar, S. N.; Tawre, M. S.; Pardesi, K. R. Emerging strategies to combat ESKAPE pathogens in the era of antimicrobial resistance: A review. *Front. Microbiol.* **2019**, *10*, 539.

(7) Farooq, M.; Mayakrishnan, G.; Kim, I. S. Photo reduced molybdenum oxide/polyacrylonitrile composite membrane for eco-friendly silver, copper ions reduction and release mechanisms. *Chem. Eng. J.* **2024**, *484*, 149219.

(8) Thakur, R. A.; Florek, C. A.; Kohn, J.; Michniak, B. B. Electrospun nanofibrous polymeric scaffold with targeted drug release profiles for potential application as wound dressing. *Int. J. Pharm.* **2008**, *364* (1), 87−93.

(9) Li, M.; Liang, Y.; He, J.; Zhang, H.; Guo, B. Two-Pronged Strategy of Biomechanically Active and Biochemically Multifunctional Hydrogel Wound Dressing To Accelerate Wound Closure and Wound Healing. *Chem. Mater.* **2020**, *32* (23), 9937−9953.

(10) Salvo, J.; Sandoval, C. Role of copper nanoparticles in wound healing for chronic wounds: Literature review. *Burns Trauma* **2022**, *10*, tkab047.

(11) Kornblatt, A. P.; Nicoletti, V. G.; Travaglia, A. The neglected role of copper ions in wound healing. *J. Inorg. Biochem.* **2016**, *161*, 1−8.

(12) Parani, M.; Lokhande, G.; Singh, A.; Gaharwar, A. K. Engineered Nanomaterials for Infection Control and Healing Acute and Chronic Wounds. *ACS Appl. Mater. Interfaces* **2016**, *8* (16), 10049−10069.

(13) Barbier-Chassefière, G.; Garcia-Filipe, S.; Yue, X. L.; Kerros, M. E.; Petit, E.; Kern, P.; Saffar, J. L.; Papy-Garcia, D.; Caruelle, J. P.; Barritault, D. Matrix therapy in regenerative medicine, a new approach to chronic wound healing. *J. Biomed. Mater. Res., Part A* **2009**, *90A* (3), 641−647.

(14) Aguirre, A.; González, A.; Navarro, M.; Castaño, Ó.; Planell, J. A.; Engel, E. Control of microenvironmental cues with a smart biomaterial composite promotes endothelial progenitor cell angiogenesis. *Eur. Cell Mater.* **2012**, *24*, 90−106.

(15) Farooq, M.; Bilal, M. I.; Gohar, S.; Khalid, M.; Haider, M. K.; Kim, I. S. Antibacterial Activity of Molybdenum Oxide−Polyacrylonitrile Composite Membrane with Fast Silver Ion Reduction. *ACS Omega* **2023**, *8* (51), 49467−49477.

(16) Farooq, M.; Khalid, M.; Yoshinori, Y.; Wang, F.; Iqbal, M. A.; Sarwar, M. N.; Mayakrishnan, G.; Kim, I. S. Ag and MoO3 Nanoparticle-Containing Polyacrylonitrile Nanofiber Membranes for Wound Dressings. *ACS Appl. Nano Mater.* **2023**, *6* (18), 17171−17178.

(17) Li, J.; Zhai, D.; Lv, F.; Yu, Q.; Ma, H.; Yin, J.; Yi, Z.; Liu, M.; Chang, J.; Wu, C. Preparation of copper-containing bioactive glass/eggshell membrane nanocomposites for improving angiogenesis, antibacterial activity and wound healing. *Acta Biomater.* **2016**, *36*, 254−266.

(18) Grzybowski, J.; Janiak, M. K.; Oidak, E.; Lasocki, K.; Wrembel-Wargocka, J.; Cheda, A.; Antos-Bielska, M.; Pojda, Z. New cytokine dressings. II. Stimulation of oxidative burst in leucocytes in vitro and reduction of viable bacteria within an infected wound. *Int. J. Pharm.* **1999**, *184* (2), 179−187.

(19) Borkow, G.; Melamed, E. Copper, an abandoned player returning to the wound healing battle, *Recent Adv. Wound Healing*, **2021**, .

(20) Cui, H.; Liu, M.; Yu, W.; Cao, Y.; Zhou, H.; Yin, J.; Liu, H.; Que, S.; Wang, J.; Huang, C.; Gong, C.; Zhao, G. Copper Peroxide-Loaded Gelatin Sponges for Wound Dressings with Antimicrobial and Accelerating Healing Properties. *ACS Appl. Mater. Interfaces* **2021**, *13* (23), 26800−26807.

(21) Qiao, Y.; Ping, Y.; Zhang, H.; Zhou, B.; Liu, F.; Yu, Y.; Xie, T.; Li, W.; Zhong, D.; Zhang, Y.; Yao, K.; Santos, H. A.; Zhou, M. Laser-Activatable CuS Nanodots to Treat Multidrug-Resistant Bacteria and Release Copper Ion to Accelerate Healing of Infected Chronic

Nonhealing Wounds. *ACS Appl. Mater. Interfaces* **2019**, *11* (4), 3809−3822.
(22) Ghasemian Lemraski, E.; Jahangirian, H.; Dashti, M.; Khajehali, E.; Sharafinia, S.; Rafiee-Moghaddam, R.; Webster, T. J. Antimicrobial double-layer wound dressing based on chitosan/polyvinyl alcohol/copper: In vitro and in vivo assessment. *Int. J. Nanomed.* **2021**, *16*, 223−235.
(23) Wu, C.; Zhou, Y.; Xu, M.; Han, P.; Chen, L.; Chang, J.; Xiao, Y. Copper-containing mesoporous bioactive glass scaffolds with multifunctional properties of angiogenesis capacity, osteostimulation and antibacterial activity. *Biomaterials* **2013**, *34* (2), 422−433.
(24) Sandoval, C.; Rios, G.; Sepulveda, N.; Salvo, J.; Souza-Mello, V.; Farias, J. Effectiveness of copper nanoparticles in wound healing process using in vivo and in vitro studies: A systematic review. *Pharmaceutics* **2022**, *14* (9), 1838.
(25) Ahmed, Z.; Briden, A.; Hall, S.; Brown, R. A. Stabilisation of cables of fibronectin with micromolar concentrations of copper: In vitro cell substrate properties. *Biomaterials* **2004**, *25* (5), 803−812.
(26) Zhang, Z.; Xue, H.; Xiong, Y.; Geng, Y.; Panayi, A. C.; Knoedler, S.; Dai, G.; Shahbazi, M. A.; Mi, B.; Liu, G. Copper incorporated biomaterial-based technologies for multifunctional wound repair. *Theranostics* **2024**, *14* (2), 547.
(27) Venkataprasanna, K. S.; Prakash, J.; Vignesh, S.; Bharath, G.; Venkatesan, M.; Banat, F.; Sahabudeen, S.; Ramachandran, S.; Devanand Venkatasubbu, G. Fabrication of Chitosan/PVA/GO/CuO patch for potential wound healing application. *Int. J. Biol. Macromol.* **2020**, *143*, 744−762.
(28) Das, M.; Goswami, U.; Kandimalla, R.; Kalita, S.; Ghosh, S. S.; Chattopadhyay, A. Iron−Copper Bimetallic Nanocomposite Reinforced Dressing Materials for Infection Control and Healing of Diabetic Wound. *ACS Appl. Biomater.* **2019**, *2* (12), 5434−5445.
(29) Ma, D. L.; He, H. Z.; Leung, K. H.; Chan, D. S. H.; Leung, C. H. Bioactive luminescent transition-metal complexes for biomedical applications. *Angew. Chem., Int. Ed.* **2013**, *52* (30), 7666−7682.
(30) Shiju, C.; Arish, D.; Kumaresan, S. Novel water soluble Schiff base metal complexes: Synthesis, characterization, antimicrobial-, DNA cleavage, and anticancer activity. *J. Mol. Struct.* **2020**, *1221*, 128770.
(31) Salah, I.; Parkin, I. P.; Allan, E. Copper as an antimicrobial agent: Recent advances. *RSC Adv.* **2021**, *11* (30), 18179−18186.
(32) Bisht, N.; Dwivedi, N.; Kumar, P.; Venkatesh, M.; Yadav, A. K.; Mishra, D.; Dhand, C.; Verma, N. K.; Lakshminarayanan, R.; Ramakrishna, S.; Mondal, D. P. Recent advances in copper and copper-derived materials for antimicrobial resistance and infection control. *Curr. Opin. Biomed. Eng.* **2022**, *24*, 100408.
(33) Nakahata, D. H.; de Paiva, R. E.; Lustri, W. R.; Corbi, P. P. Sulfonamide-containing copper (ii) complexes: New insights on biophysical interactions and antibacterial activities. *New J. Chem.* **2020**, *44* (40), 17236−17244.
(34) Ahire, J. J.; Hattingh, M.; Neveling, D. P.; Dicks, L. M. Copper-containing anti-biofilm nanofiber scaffolds as a wound dressing material. *PLoS One* **2016**, *11* (3), No. e0152755.
(35) Shrestha, S.; Wang, B.; Dutta, P. K. Commercial Silver-Based Dressings: In Vitro and Clinical Studies in Treatment of Chronic and Burn Wounds. *Antibiotics* **2024**, *13* (9), 910.
(36) Gámez-Herrera, E.; García-Salinas, S.; Salido, S.; Sancho-Albero, M.; Andreu, V.; Pérez, M.; Luján, L.; Irusta, S.; Arruebo, M.; Mendoza, G. Drug-eluting wound dressings having sustained release of antimicrobial compounds. *Eur. J. Pharm. Biopharm.* **2020**, *152*, 327−339.
(37) Zupančič, Š.; Preem, L.; Kristl, J.; Putrinš, M.; Tenson, T.; Kocbek, P.; Kogermann, K. Impact of PCL nanofiber mat structural properties on hydrophilic drug release and antibacterial activity on periodontal pathogens. *Eur. J. Pharm. Sci.* **2018**, *122*, 347−358.
(38) Mia, R.; Khan, M. T.; Al Mamun, M. A.; Xu, A.; Rashid, M. M. Effect of different solvent systems on fiber morphology and property of electrospun PCL nano fibers. *J. Text. Eng.* **2021**, *28* (122), 61−76.
(39) Capello, C.; Fischer, U.; Hungerbühler, K. What is a green solvent? A comprehensive framework for the environmental assessment of solvents. *Green Chem.* **2007**, *9* (9), 927−934.
(40) Stepping, S. M.; Vashistha, N.; Ullah, S.; Liu, P.; Anjass, M.; Dietzek-Ivanšić, B. Reductive quenching of photosensitizer [Ru (bpy) 3] 2+ reveals the inhomogeneous distribution of sites in PAN polymer nanofibers for light-driven redox catalysis. *RSC Adv.* **2024**, *14* (44), 32501−32505.
(41) Bozkaya, O.; Arat, E.; Gün Gök, Z.; Yiğitoğlu, M.; Vargel, I. Production and characterization of hybrid nanofiber wound dressing containing Centella asiatica coated silver nanoparticles by mutual electrospinning method. *Eur. Polym. J.* **2022**, *166*, 111023.
(42) Ahmadi Bonakdar, M.; Rodrigue, D. Electrospinning: Processes, structures, and materials. *Macromol* **2024**, *4* (1), 58−103.
(43) Ghasemi-Mobarakeh, L.; Prabhakaran, M. P.; Morshed, M.; Nasr-Esfahani, M.-H.; Ramakrishna, S. Electrospun poly(ϵ-caprolactone)/gelatin nanofibrous scaffolds for nerve tissue engineering. *Biomaterials* **2008**, *29* (34), 4532−4539.
(44) Catledge, S. A.; Clem, W. C.; Shrikishen, N.; Chowdhury, S.; Stanishevsky, A. V.; Koopman, M.; Vohra, Y. K. An electrospun triphasic nanofibrous scaffold for bone tissue engineering. *Biomed. Mater.* **2007**, *2* (2), 142.
(45) Baji, A.; Mai, Y. W.; Wong, S. C.; Abtahi, M.; Chen, P. Electrospinning of polymer nanofibers: Effects on oriented morphology, structures and tensile properties. *Compos. Sci. Technol.* **2010**, *70* (5), 703−718.
(46) Solano, A. G. R.; de Fátima Pereira, A.; Pinto, F. C. H.; Ferreira, L. G. R.; de Oliveira Barbosa, L. A.; Fialho, S. L.; de Oliveira Patricio, P. S.; da Silva Cunha, A.; da Silva, G. R.; Pianetti, G. A. Development and evaluation of sustained-release etoposide-loaded poly (ϵ-caprolactone) implants. *AAPS Pharm. Sci. Technol.* **2013**, *14*, 890−900.
(47) Rathinavel, S.; Korrapati, P. S.; Kalaiselvi, P.; Dharmalingam, S. Mesoporous silica incorporated PCL/Curcumin nanofiber for wound healing application. *Eur. J. Pharm. Sci.* **2021**, *167*, 106021.
(48) Li, R.; Song, Y.; Fouladian, P.; Arafat, M.; Chung, R.; Kohlhagen, J.; Garg, S. Three-dimensional printing of curcumin-loaded biodegradable and flexible scaffold for intracranial therapy of glioblastoma multiforme. *Pharmaceutics* **2021**, *13* (4), 471.
(49) Elabbasy, M. T.; Atteya, M. R.; Samak, M. A.; Abdelrahman, M.; AlMahmoud, T.; El-Morsy, M. A.; Menazea, A. A.; Abd El-Kader, M. F. H. Dysprosium oxide, alumina, and graphene oxide reinforced polycaprolactone thin films: Thermal stability, morphology, and cell viability. *J. Rare Earth* **2024**, *42* (7), 1337−1343.
(50) Chakrapani, V. Y.; Gnanamani, A.; Giridev, V. R.; Madhusoothanan, M.; Sekaran, G. Electrospinning of type I collagen and PCL nanofibers using acetic acid. *J. Appl. Polym. Sci.* **2012**, *125* (4), 3221−3227.
(51) Yang, J.; Xu, L. Electrospun nanofiber membranes with various structures for wound dressing. *Materials* **2023**, *16* (17), 6021.
(52) Bodón, J. S.; Galbarriatu, M. D.; Pérez, L.; Moreno, I.; Vilas, J. L. Strategies to enhance biomedical device performance and safety: A comprehensive review. *Coatings* **2023**, *13* (12), 1981.
(53) Yang, Y.; Du, Y.; Zhang, J.; Zhang, H.; Guo, B. Structural and functional design of electrospun nanofibers for hemostasis and wound healing. *Adv. Fiber Mater.* **2022**, *4* (5), 1027−1057.
(54) Huang, Y.; Dan, N.; Dan, W.; Zhao, W. Reinforcement of Polycaprolactone/Chitosan with Nanoclay and Controlled Release of Curcumin for Wound Dressing. *ACS Omega* **2019**, *4* (27), 22292−22301.
(55) Wang, J.; Planz, V.; Vukosavljevic, B.; Windbergs, M. Multifunctional electrospun nanofibers for wound application−Novel insights into the control of drug release and antimicrobial activity. *Eur. J. Pharm. Biopharm.* **2018**, *129*, 175−183.
(56) Saghazadeh, S.; Rinoldi, C.; Schot, M.; Kashaf, S. S.; Sharifi, F.; Jalilian, E.; Nuutila, K.; Giatsidis, G.; Mostafalu, P.; Derakhshandeh, H.; Yue, K.; Swieszkowski, W.; Memic, A.; Tamayol, A.; Khademhosseini, A. Drug delivery systems and materials for wound healing applications. *Adv. Drug Delivery Rev.* **2018**, *127*, 138−166.

https://doi.org/10.1021/acsomega.4c09305
ACS Omega 2025, 10, 12961−12971

(57) Sultanova, Z.; Kaleli, G.; Kabay, G.; Mutlu, M. Controlled release of a hydrophilic drug from coaxially electrospun polycaprolactone nanofibers. *Int. J. Pharm.* **2016**, *505* (1), 133−138.
(58) Kamaly, N.; Yameen, B.; Wu, J.; Farokhzad, O. C. Degradable controlled-release polymers and polymeric nanoparticles: Mechanisms of controlling drug release. *Chem. Rev.* **2016**, *116* (4), 2602−2663.
(59) Spizzirri, U. G. Functional polymers for controlled drug release. *Pharmaceutics* **2020**, *12* (2), 135.
(60) Santadkha, T.; Skolpap, W.; Thitapakorn, V. Diffusion Modeling and in vitro release kinetics studies of curcumin− loaded superparamagnetic nanomicelles in cancer drug delivery system. *J. Pharm. Sci.* **2022**, *111* (6), 1690−1699.
(61) Permanadewi, I.; Kumoro, A. C.; Wardhani, D. H.; Aryanti, N. Modelling of controlled drug release in gastrointestinal tract simulation. In *Journal of Physics: conference Series*; IOP Publishing, 2019; Vol. *1295*(1), pp. 012063
(62) Lee, J. S.; Lee, H. B.; Oh, Y.; Choi, A.-J.; Seo, T. H.; Kim, Y.-K.; Lee, M. W. Used coffee/PCL composite filter for Cu(II) removal from wastewater. *J. Water Process. Eng.* **2022**, *50*, 103253.
(63) Shoba, E.; Lakra, R.; Kiran, M. S.; Korrapati, P. S. Fabrication of core−shell nanofibers for controlled delivery of bromelain and salvianolic acid B for skin regeneration in wound therapeutics. *Biomed. Mater.* **2017**, *12* (3), 35005.
(64) Yildiz, S. C.; Demir, C.; Cengiz, M.; Ayhanci, A. Protective properties of kefir on burn wounds of mice that were infected with S. aureus, P. auroginasa and *E. coli*. *Cell Mol. Biol.* **2019**, *65* (7), 60−65.
(65) Alavarse, A. C.; de Oliveira Silva, F. W.; Colque, J. T.; da Silva, V. M.; Prieto, T.; Venancio, E. C.; Bonvent, J.-J. Tetracycline hydrochloride-loaded electrospun nanofibers mats based on PVA and chitosan for wound dressing. *Mater. Sci. Eng., C* **2017**, *77*, 271−281.
(66) Zuo, Z.; Pan, X.; Yang, G.; Zhang, Y.; Liu, X.; Zha, J.; Yuan, X. Cu (I) complexes with aggregation-induced emission for enhanced photodynamic antibacterial application. *Dalton Trans.* **2023**, *52* (10), 2942−2947.
(67) Kalayil, N.; Budar, A. A.; Dave, R. K. Nanofibers for Drug Delivery: Design and Fabrication Strategies. *BIO Integration* **2024**, *5* (1), 978.

https://doi.org/10.1021/acsomega.4c09305
ACS Omega 2025, 10, 12961−12971